Dyes and Pigments 83 (2009) 249–257

Contents lists available at ScienceDirect

Dyes and Pigments

journal homepage: www.elsevier.com/locate/dyepig

The binding of C.I. Acid Red 2 to human serum albumin: Determination of binding mechanism and binding site using fluorescence spectroscopy

Fei Ding [a], Nan Li [a], Binyue Han [b], Feng Liu [a], Li Zhang [a], Ying Sun [a,*]

[a] Department of Chemistry, China Agricultural University, No. 2 Yuanmingyuan Xi Road Haidian District, Beijing 100193, China
[b] College of Biological Sciences, China Agricultural University, Beijing 100193, China

ARTICLE INFO

Article history:
Received 3 February 2009
Received in revised form
10 May 2009
Accepted 12 May 2009
Available online 27 May 2009

Keywords:
C.I. Acid Red 2
Human serum albumin
Fluorescence quenching
Site competitive binding
Circular dichroism
Thermodynamic parameter

ABSTRACT

The mechanism of interaction between C.I. Acid Red 2 and human serum albumin was studied using different spectroscopic methods. The binding constants for the formation of a complex between the dye and albumin were 2.557, 2.461 and 2.383 $\times$ 10^5 M^{-1} at 298, 304 and 310 K, respectively. The associated changes in enthalpy and entropy were -4.512 kJ mol^{-1} and 88.38 J mol^{-1} K^{-1}, indicating that hydrophobic interactions as well as H-bonding were the dominant intermolecular forces stabilizing the complex. Site marker competitive experiments revealed that the binding of the dye to albumin occurred in subdomain IIA; the distance between dye and albumin was 3.91 nm according to fluorescence resonance energy transfer theory. Changes in the albumin secondary structure imparted by the dye were confirmed using synchronous fluorescence, electronic absorption, circular dichroism and three-dimensional fluorescence spectroscopy.

1. Introduction

Azo dyes make up the largest and most versatile class of dyes with more than 2000 different azo dyes being currently used. More than 8.0 $\times$ 10^8 kg of dyes are annually produced worldwide, of which 60–70% are azo dyes [1,2]. They are characterized by one or more azo groups (–*N*═*N*–) in their chemical structure and can be used to color a large number of different substrates, such as textiles, papers, leathers, gasoline, additives, foodstuffs and cosmetics [3]. It has been estimated that over 10% of the dyes are lost to the environment in the effluent during dyeing processes. Moreover, some azo colorants have been related to bladder cancer in humans, to splenic sarcomas, hepatocarcinomas and nuclear anomalies in experimental animals, and to chromosomal aberrations in mammalian cells [4,5]. As azo dye at any level is harmful to human beings, so it has been classified as a kind of carcinogen by the European Union Commission [6]. Due to their potential carcinogenicity, the German government has recently banned the imports of textiles, leathers and other items dyed with azo dyes [7]. C.I. Acid Red 2 (2-[4-(dimethylamino)phenylazo] benzoic acid, structure shown in Fig. 1) is a well-known azo dye and has been extensively used in textile dyeing and paper printing [8]; however, it causes eye and skin irritation and irritation of respiratory and digestive tract if inhaled/swallowed. It is also a suspected carcinogen and mutagen [9].

Transportation, distribution, physiological and toxicological actions of dyes *in vivo* are closely related to their binding with proteins, so the investigation of dyes with respect to protein–dye binding is imperative and of fundamental importance. Human serum albumin (HSA) is the most abundant protein constituent of blood plasma and has been used as a model protein for many and diverse biophysical and physicochemical studies [10]. He and Carter [11] have determined the three-dimensional structure of HSA through X-ray crystallographic measurements. The globular protein consists of three homologous domains that assemble to form a heart-shaped molecule, each domain contains two subdomains (A and B), and is stabilized by 17 disulfide bridges. Aromatic and heterocyclic ligands were found to bind within two hydrophobic pockets in subdomains IIA and IIIA, which are consistent with site I and site II. Site I is formed as a pocket in subdomain IIA and involves the lone tryptophan of the protein (Trp-214). Site II corresponds to the pocket of subdomain IIIA, which is almost the same size as site I, the interior of cavity is constituted of hydrophobic amino acid residues (Arg-410 and Tyr-411) [12,13]. In plasma, this protein is able to bind, and thereby transport, various substances such as amino acids, fatty acids, hormones, drugs and dyes [14]. It is well-known that the remarkable binding properties of HSA accounts for the central role in both the toxicity and rate of delivery of dyes. In

* Corresponding author. Tel./fax: +86 10 62737071.
E-mail addresses: caulizhang@yeah.net (L. Zhang), sunying@cau.edu.cn (Y. Sun).

0143-7208/$ – see front matter © 2009 Elsevier Ltd. All rights reserved.
doi:10.1016/j.dyepig.2009.05.003

addition, there is evidence of conformation changes of HSA induced by its interaction with dyes, which appears to affect the secondary and tertiary structure of HSA [15,16]. Consequently, the investigation on the interaction of dyes to HSA is of great importance. Shaikh et al. have studied the binding of bromopyrogallol red and rose bengal to BSA in order to investigate their high affinity to BSA [17,18]. Yue et al. have studied the binding of C.I. Direct Yellow 9 to HSA [19]. A spectrophotometric method has been developed for the determination of C.I. Acid Red 2-protein adducts [20,21], yet other parameters like mode of interaction, binding mechanism and binding site are also important, these investigation may provide major theoretical information for the improvement of the metabolism and distribution of C.I. Acid Red 2 in life sciences, biological techniques and molecular functional design. Furthermore, to our knowledge, the investigation of C.I. Acid Red 2 interaction with HSA using fluorescence spectroscopy is the first report of this type of analysis.

In this paper, the interaction between C.I. Acid Red 2 and HSA was studied under physiological conditions by fluorescence, electronic absorption and circular dichroism (CD) spectroscopy. Great attempts were made to investigate the binding mechanism between them regarding the quenching mechanism, the specific binding site, the type of binding force and the effect of C.I. Acid Red 2 on the secondary structure changes of HSA. This work cannot only provide valuable information for the transportation and distribution of C.I. Acid Red 2, but also illustrate the mechanism of interaction of azo dyes with protein.

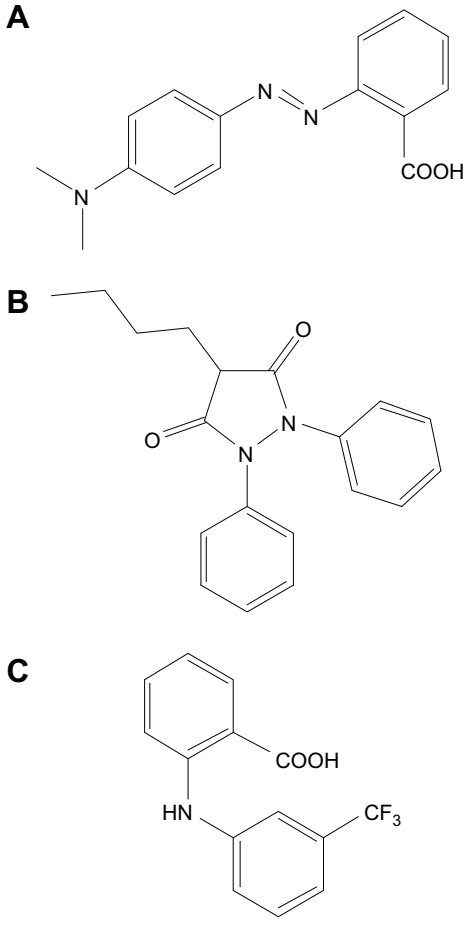

Fig. 1. Chemical structure of C.I. Acid Red 2 (A), phenylbutazone (B) and flufenamic acid (C).

2. Materials and methods

2.1. Materials

Human serum albumin (fatty acid free < 0.05%) and C.I. Acid Red 2 (CAS: 493-52-7) were purchased from Sigma–Aldrich Chemical Company. All other reagents were of analytical grade reagent. Milli-Q ultrapure water was used throughout the experiments. NaCl (1.0 M) solution was used to maintain the ionic strength at 0.1. Tris (0.2 M)–HCl (0.1 M) was used to keep the pH of the solution at 7.4. Dilutions of the HSA stock (1.0×10^{-5} M) in Tris–HCl buffer solution were prepared immediately before use. The concentration of HSA was determined spectrophotometrically using $E_{1\ cm}^{1\%}$ of 5.30 at 280 nm [22]. The stock solution (5.0×10^{-4} M) of C.I. Acid Red 2 was prepared in absolute ethanol.

2.2. Fluorescence and electronic absorption spectra

Fluorescence spectra were performed on an F-4500 spectrofluorimeter (Hitachi, Japan) equipped with 1.0 cm quartz cell and a thermostat bath. Fluorescence emission spectra were recorded at 298, 304 and 310 K in the range of 290–500 nm. The width of the excitation and emission slit was set to 5.0 and 5.0 nm, respectively. An excitation wavelength of 295 nm was chosen and very dilute solutions were used in the experiment (HSA 1.0×10^{-6} M, C.I. Acid Red 2 in the range of 0–14.4×10^{-6} M) to avoid the inner filter effect. The quenching effect of ethanol was evaluated and the result indicated that there was almost no influence of ethanol on the C.I. Acid Red 2–HSA interaction.

Site marker competitive experiments: The concentration of HSA and phenylbutazone/flufenamic acid were all stabilized at 1.0×10^{-6} M C.I. Acid Red 2 was then gradually added to the HSA–phenylbutazone or HSA–flufenamic acid mixtures. An excitation wavelength of 295 nm was selected and the fluorescence spectra were recorded in the range of 290–500 nm.

The three-dimensional fluorescence spectra were performed under the following conditions: the emission wavelength was recorded between 200 and 500 nm, the initial excitation wavelength was set to 200 nm with increment of 10 nm, the number of scanning curves was 16, and other scanning parameters were identical to those of the fluorescence emission spectra.

Electronic absorption spectra were recorded at room temperature on a Cary-100 spectrophotometer (Varian, USA) equipped with 1.0 cm quartz cuvette. The wavelength range was from 200 to 400 nm.

CD spectra were recorded with a Jasco-810 spectropolarimeter (Jasco, Japan) using a 0.1 cm path length quartz cell. Measurements were taken at wavelengths between 200 and 250 nm with 0.2 nm step resolution and averaged over five scans recorded as a speed of 50 nm min^{-1}. All observed CD spectra were baseline subtracted for buffer and the helicity was calculated from the molar ellipticity ([e], deg cm^2 $dmol^{-1}$) value at 222 nm using the following equation [23]:

$$\%\alpha - \text{helix} = \frac{-[e]_{222} - 2,340}{30,300} \quad (1)$$

3. Results and discussion

3.1. Effect of ethanol

The ethanol alone effect on the fluorescence spectra of HSA in the pH 7.4 Tris–HCl buffer were measured with the excitation wavelength at 295 nm and the results are shown in Fig. 2. As can be seen from Fig. 2, the effect of ethanol on the fluorescence intensity

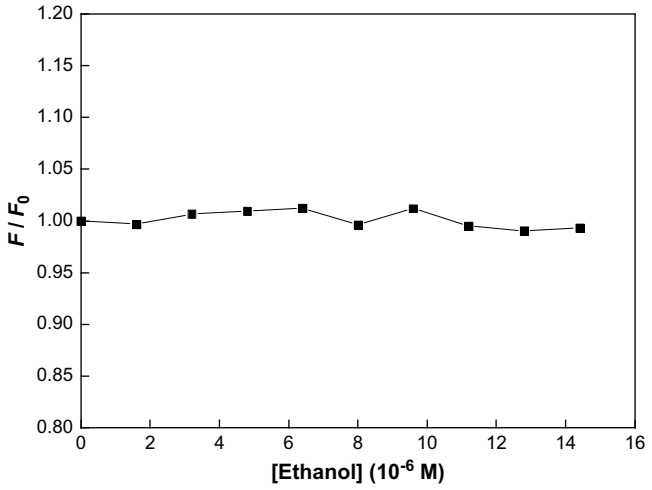

Fig. 2. Effect of ethanol on the fluorescence intensity of HSA. c(HSA) = 1.0 × 10^{-6} M, c(ethanol) = 0, 1.6, 3.2, 4.8, 6.4, 8.0, 9.6, 11.2, 12.8, 14.4 × 10^{-6} M pH = 7.4, T = 298 K.

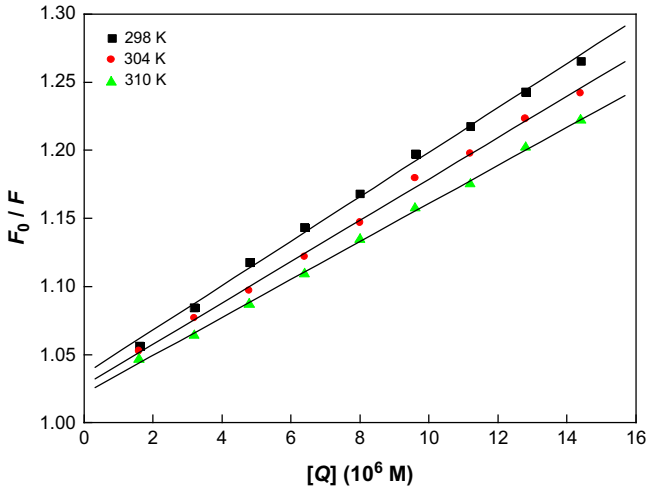

Fig. 4. Stern–Volmer plots for the C.I. Acid Red 2–HSA system at three different temperatures. c(HSA) = 1.0 × 10^{-6} M; pH = 7.4.

of HSA could be negligible. In other words, there was almost no influence of ethanol on the HSA conformation.

3.2. Fluorescence quenching mechanism

The fluorescence intensity of a compound can be decreased by a variety of molecular interactions, such as excited-state reactions, molecular rearrangements, energy transfer, ground-state complex formation and collision quenching [24]. Such a decrease in intensity is called fluorescence quenching. Fig. 3 shows the fluorescence emission spectra of HSA with various amounts of C.I. Acid Red 2 following excitation at 295 nm. This excitation wavelength avoids excitation of tyrosine (Tyr) and selectively excites tryptophan (Trp). As can be seen from Fig. 3, the fluorescence intensity of HSA decreased regularly and there was almost no shift of the emission wavelength with the addition of C.I. Acid Red 2. Under the same conditions, no fluorescence of C.I. Acid Red 2 was observed. These results implied that interaction between dye and HSA occurs resulting in quenching the intrinsic fluorescence of HSA [25].

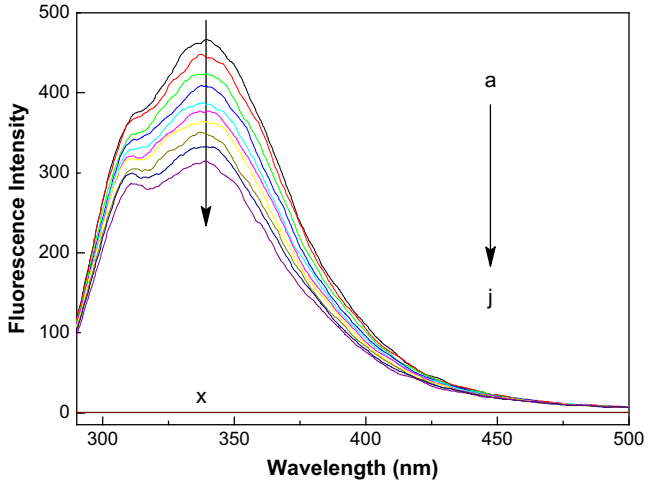

Fig. 3. The fluorescence spectra of C.I. Acid Red 2–HSA system. (a) 1.0 × 10^{-6} M HSA; (b→j) 1.0 × 10^{-6} M HSA in the presence of 1.6, 3.2, 4.8, 6.4, 8.0, 9.6, 11.2, 12.8, 14.4 × 10^{-6} M C.I. Acid Red 2; (×) 14.4 × 10^{-6} M C.I. Acid Red 2. pH = 7.4, T = 298 K.

Fluorescence quenching of HSA results from a decrease of fluorescence quantum yield. The Stern–Volmer equation is often applied to describe the fluorescence quenching and analyze the quenching mechanism [26]:

$$\frac{F_0}{F} = 1 + K_{SV}[Q] = 1 + k_q\tau_0[Q] \quad (2)$$

where F_0 and F are the fluorescence intensities before and after the addition of the quencher. k_q, K_{SV}, τ_0 and [Q] are the quenching rate constant of the biomolecule, the Stern–Volmer dynamic quenching constant, the average lifetime of the molecule without quencher (τ_0 = 10^{-8} s [27]) and the concentration of the quencher, respectively. Fig. 4 shows the Stern–Volmer plots of F_0/F *versus* [Q] at three different temperatures and the calculated K_{SV} and k_q values are summarized in Table 1. The results revealed that the Stern–Volmer dynamic quenching constant K_{SV} and k_q is inversely correlated with increasing temperature and the values of k_q were much greater than the maximum scatter collision quenching constant of various quenchers (2.0 × 10^{10} M^{-1} s^{-1} [28]), which indicated that the probable quenching mechanism of dye–HSA interaction was not initiated by dynamic collision but compound formation [29]. That is, the dye is bound to HSA and a dye–HSA complex is formed, which resulted in a fluorescence quenching of the fluorophore.

Therefore, the quenching data were examined according to the Lineweaver–Burk equation [14]:

$$\frac{1}{F_0 - F} = \frac{1}{F_0} + \frac{1}{K_a F_0[Q]} \quad (3)$$

where K_a denotes the binding constant of dye and HSA, which can be calculated from the slope and intercept of Lineweaver–Burk curves as shown in Fig. 5, and the corresponding results of K_a values at different temperatures are listed in Table 2. The decreasing trend

Table 1
Stern–Volmer quenching constants for the interaction of C.I. Acid Red 2 with HSA at three different temperatures.

T (K)	K_{SV} (× 10^4 M^{-1})	k_q (× 10^{12} M^{-1} s^{-1})	R[a]	S.D.[b]
298	1.631	1.631	0.9985	0.004
304	1.516	1.516	0.9989	0.004
310	1.395	1.395	0.9994	0.003

[a] R is the correlation coefficient.
[b] S.D. is the standard deviation.

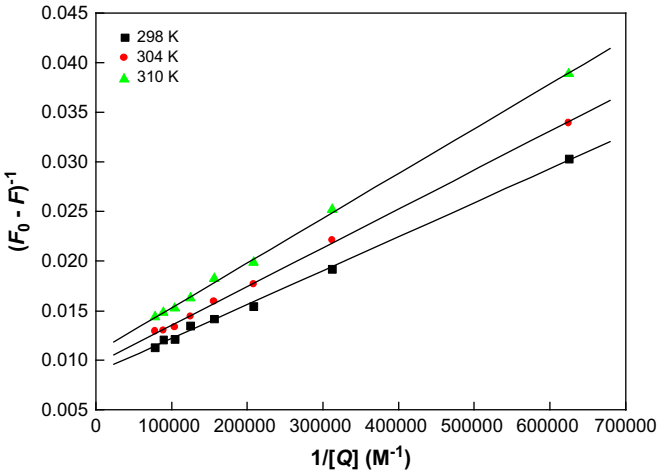

Fig. 5. Lineweaver–Burk plots for the C.I. Acid Red 2–HSA at different temperatures. c(HSA) = 1.0 × 10^{-6} M; pH = 7.4.

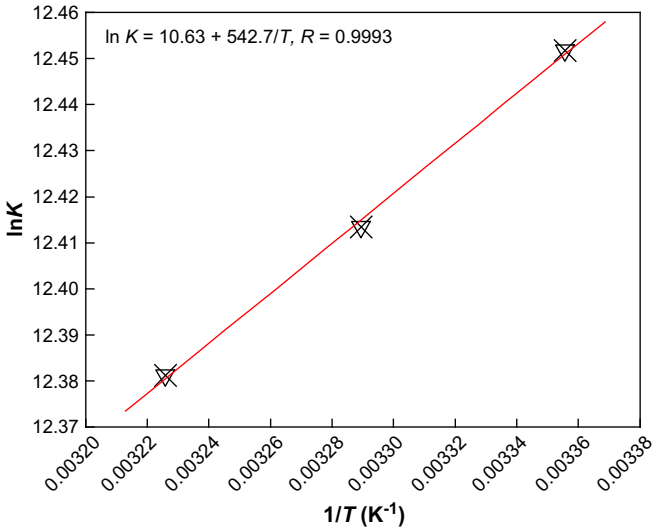

Fig. 6. Van't Hoff plot for the interaction of HSA and C.I. Acid Red 2 in Tris–HCl buffer, pH = 7.4.

of K_a with increasing temperature was in accordance with the dependence of K_{SV} on temperature as mentioned above. In previous work, fluorescence titration experiments have shown that other azo dyes binding to HSA have binding constants of 2.55 × 10^7 M^{-1} [30] and 2.14 × 10^8 M^{-1} [31], respectively. Moreover, most ligands are bound reversibly and display moderate affinities for albumins (binding constants in the range 1–20.5 × 10^5 M^{-1} [32]). Therefore, in the present work, the binding constant between dye and HSA is moderate and C.I. Acid Red 2 can be stored and carried by HSA in the body [33].

3.3. Binding mode

The acting forces between a small molecule and macromolecule mainly include hydrogen bonds, van der Waals forces, electrostatic forces and hydrophobic interactions [34]. The thermodynamic parameters, enthalpy change (ΔH), entropy change (ΔS) and free energy change (ΔG) are the main characteristics to determine the binding mode. The temperatures chosen for measurements were 298, 304 and 310 K so that HSA does not undergo any structural degradation. The thermodynamic parameters can be calculated from the van't Hoff equation:

$$\ln K^{\Theta} = \frac{-\Delta H^{\Theta}}{RT} + \frac{\Delta S^{\Theta}}{R} \quad (4)$$

K is analogous to the binding constants K_a and R is gas constant. The value of ΔH and ΔS were obtained from linear van't Hoff plot. The value of ΔG was calculated from the equation:

$$\Delta G^{\Theta} = \Delta H^{\Theta} - T\Delta S^{\Theta} \quad (5)$$

From the linear relationship between ln K and the reciprocal absolute temperature (Fig. 6), the value of ΔH, ΔS and ΔG were obtained and are presented in Table 2. The negative sign for ΔG means that the binding process was spontaneous and the formation of the dye–HSA complex was an exothermic reaction accompanied by a positive ΔS value. Ross and Subramanian [35] have characterized the sign and magnitude of the thermodynamic parameter associated with various individual kinds of interaction that may take place in protein association processes. From the point of water structure, a positive ΔS value is frequently taken as evidence for a hydrophobic interaction. Furthermore, the negative ΔH value (−4.512 kJ mol^{-1}) observed cannot be mainly attributed to electrostatic interactions since for electrostatic interactions ΔH is very small, almost zero [35]. A negative ΔH value is observed whenever there is hydrogen bond in the binding. It is not possible to account for the thermodynamic parameters of the dye–HSA coordination complex on the basis of a single intermolecular force model. Consequently, the negative ΔH and positive ΔS values suggest that hydrophobic and hydrogen bond interactions play major roles in the dye–HSA binding reaction and contributed to the stability of the complex.

Table 2
Lineweaver–Burk constants K_a and relative thermodynamic parameters of the C.I. Acid Red 2–HSA system.

T (K)	K_a (× 10^5 M^{-1})	R^a	ΔH (kJ mol^{-1})	ΔG (kJ mol^{-1})	ΔS (J mol^{-1} K^{-1})
298	2.557	0.9989	−4.512	−30.85	88.38
304	2.461	0.9995		−31.37	
310	2.383	0.9995		−31.91	

[a] R is the correlation coefficient for the K_a values.

3.4. Location of binding site

When ligand molecules bind independently to a set of equivalent sites on a macromolecule, the equilibrium between free and bound molecules is given by the equation [36]:

$$\log \frac{F_0 - F}{F} = n\log K_b + n\log\left(\frac{1}{[Q_t] - \frac{F_0 - F}{F_0}[P_t]}\right) \quad (6)$$

where F_0 and F are the fluorescence intensities before and after the addition of the quencher, K_b and n are the apparent binding constant and the number of binding sites, $[Q_t]$ and $[P_t]$ are the total quencher concentration and the total HSA concentration, respectively. Thus, a plot of $\log(F_0-F)/F$ *versus* $\log(1/([Q_t]-(F_0-F)[P_t]/F_0))$ can be used to determined K_b as well as n. For the system of C.I. Acid Red 2 and HSA, the values of K_b and n at 298 K were found to be 2.564 × 10^5 M^{-1} and 1.19, respectively. The value of n was approximately equal to 1, which implied that there was one independent class of binding site for the dye towards HSA.

In order to further classify dye binding site on HSA, competitive binding experiments have been carried out, using drugs that specifically bind to a known site or region on HSA. Crystallographic

analyses have revealed that HSA consists of a single polypeptide chain of 585 amino acid residues and comprises of three structurally homologous domains (I-III): I (residues 1-195), II (196-383), III (384-585), that assemble to form a heart-shaped molecule, and each domain containing two subdomains called A and B [11]. Sudlow et al. [37] have suggested that HSA has binding sites of ligand within hydrophobic cavities in subdomains IIA and IIIA, which are consistent with site I and site II. Site I of HSA showed affinity for warfarin, phenylbutazone, etc., while site II for diazepam, flufenamic acid, etc. In this paper, the competitors used included phenylbutazone, a characteristic marker for site I, and flufenamic acid for site II.

During the site marker competitive experiment, C.I. Acid Red 2 was gradually added to the solution of HSA and site markers held in equimolar concentrations (1.0×10^{-6} M). As shown in Fig. 7(A), with addition of phenylbutazone into HSA solution, the fluorescence intensity was significantly lower than that of without phenylbutazone. Then, after adding the dye into the above system, the fluorescence intensity of HSA solution, with phenylbutazone held in equimolar, decreased gradually, and the intensity was much lower than that of without phenylbutazone, displaying that the binding of the dye to HSA was affected after adding phenylbutazone. On the contrary, in the presence of flufenamic acid, the fluorescence intensity of the dye–HSA complex almost had no difference from that recorded without flufenamic acid under the same conditions (Fig. 7(B)), which indicated that site II marker did not prevent the binding of dye in its usual binding location. According to the Lineweaver–Burk equation (3), the binding constants K_a' of the dye–HSA system with the presence of site markers were evaluated (Fig. 8) from the fluorescence data listed in Table 3. As shown in Table 3, the binding constant was remarkably decreased after addition of phenylbutazone, while the addition of flufenamic acid results in only a small difference. These results indicate that phenylbutazone can displace the dye but flufenamic acid has little effect on the binding of dye to HSA. The above experimental results and analysis demonstrated that C.I. Acid Red 2 has one reactive site of HSA, that is, the high affinity site (Sudlow's site I).

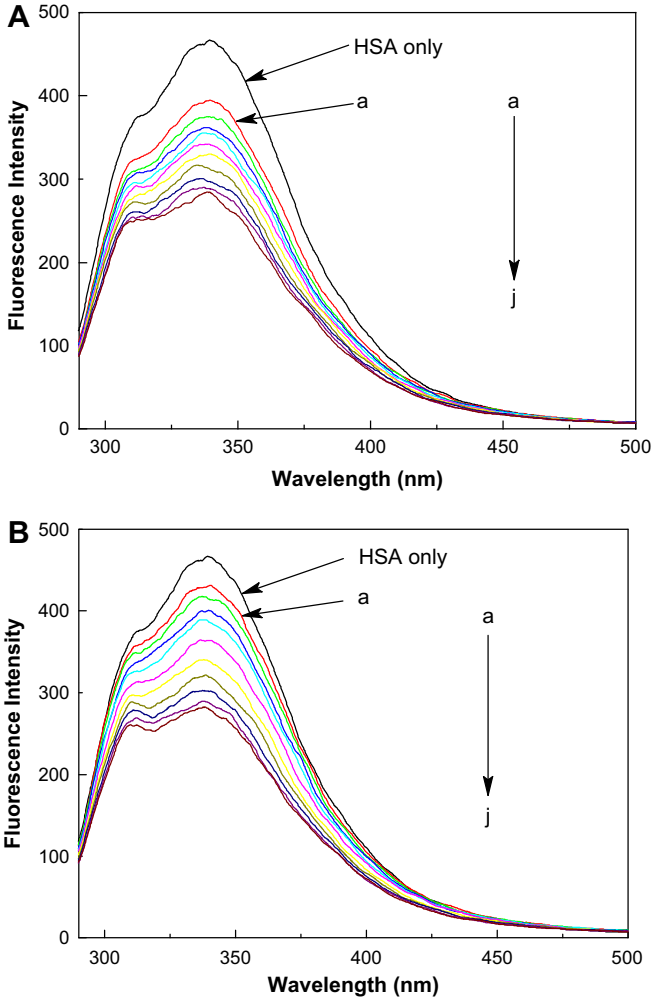

Fig. 7. Effect of site markers on the fluorescence of C.I. Acid Red 2 bound HSA. (A) c(HSA) = c(phenylbutazone) = 1.0×10^{-6} M; (B) c(HSA) = c(fluofenamic acid) = 1.0×10^{-6} M; c(C.I. Acid Red 2), a→j: 0, 1.6, 3.2, 4.8, 6.4, 8.0, 9.6, 11.2, 12.8, 14.4 $\times 10^{-6}$ M, respectively. pH = 7.4, T = 298 K.

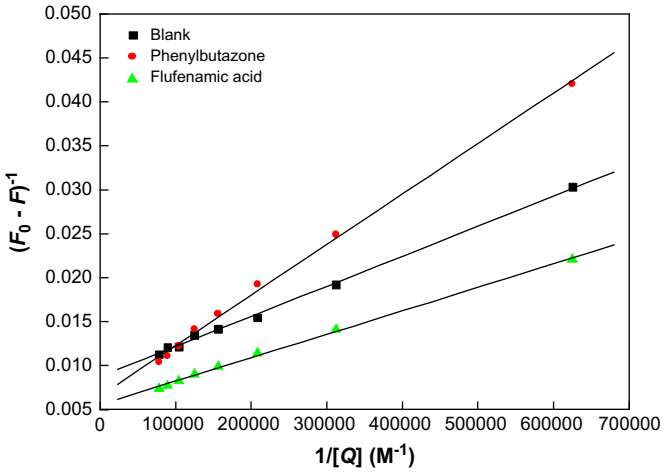

Fig. 8. Lineweaver–Burk plots for the C.I. Acid Red 2–HSA system in the presence and absence of site markers. pH = 7.4, T = 298 K.

3.5. Energy transfer

Generally, fluorescence resonance energy transfer occurs whenever the emission spectrum of a fluorophore (donor) overlaps with the absorption spectrum of another molecule (acceptor). The overlap of the absorption spectrum of the dye with the fluorescence emission spectra of HSA is shown in Fig. 9. According to fluorescence resonance energy transfer theory [38], the efficiency of the energy transfer depends on: (i) the extent of overlap of fluorescence emission spectrum of the donor with the absorption spectrum of the acceptor, (ii) the relative orientation of the donor and acceptor dipoles, and (iii) the distance between the donor and the acceptor. Here the donor and acceptor were HSA and the dye, respectively. The efficiency, E, can be calculated using the equation:

$$E = 1 - \frac{F}{F_0} = \frac{R_0^6}{R_0^6 + r^6} \tag{7}$$

where F and F_0 are the fluorescence intensities with and without dye, respectively. r is the distance between acceptor and donor, and R_0 is the critical distance when the energy transfer efficiency is 50%.

Table 3
The binding constants of competitive experiments of C.I. Acid Red 2–HSA system.

Site marker	K_a' ($\times 10^5$ M^{-1})	R[a]
Blank	2.557	0.9989
Phenylbutazone	1.136	0.9987
Flufenamic acid	2.077	0.9989

[a] R is the correlation coefficient.

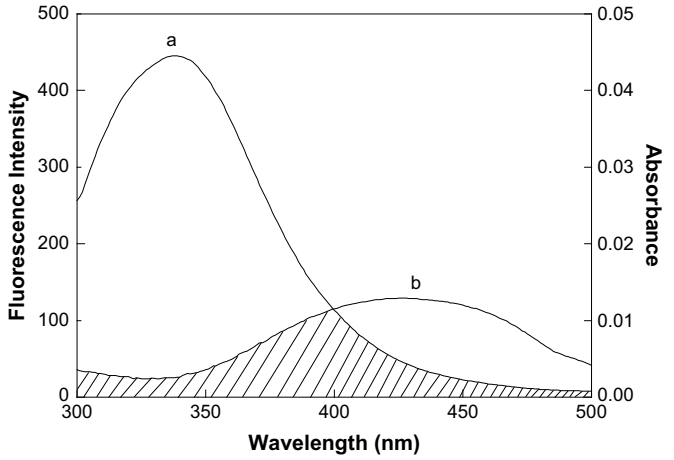

Fig. 9. Overlapping between the fluorescence emission spectrum of HSA (a) and UV/vis spectrum of C.I. Acid Red 2 (b). c(HSA) = c(C.I. Acid Red 2) = 1.0×10^{-6} M; pH = 7.4, T = 298 K.

$$R_0^6 = 8.79 \times 10^{-25} k^2 \cdot n^{-4} \cdot \varphi \cdot J \quad (8)$$

where k^2 is the spatial orientation factor of the dipole, n is the refractive index of the medium, φ is the fluorescence quantum yield of the donor and J is the overlap integral of the fluorescence emission spectrum of the donor and the absorption spectrum of the acceptor. J is given by

$$J = \frac{\sum F(\lambda)\varepsilon(\lambda)\lambda^4 \Delta\lambda}{\sum F(\lambda)\Delta\lambda} \quad (9)$$

where $F(\lambda)$ is the fluorescence intensity of the fluorescence donor of wavelength, λ, and $\varepsilon(\lambda)$ is the molar absorption coefficient of the acceptor at wavelength, λ. In the presence case, $k^2 = 2/3$, $n = 1.336$ and $\varphi = 0.118$ for HSA [19]. According to the equations (7)–(9), the values of the parameters were found to be: $J = 1.064 \times 10^{-14}$ cm^3 M^{-1}, $R_0 = 2.48$ nm, $E = 0.061$ and $r = 3.91$ nm. The donor-to-acceptor distance, $r < 7$ nm indicated that the energy transfer from HSA to dye occurs with high possibility. Further the value of r was greater than R_0 in this study which suggested that the dye could strongly quench the intrinsic fluorescence of HSA by a static quenching mechanism [39].

3.6. Conformational investigations

3.6.1. Synchronous fluorescence spectra

Synchronous fluorescence spectroscopy introduced by Lloyd [40] has been used to characterize complex mixtures providing fingerprints of complex samples. The synchronous fluorescence spectra gives information about the molecular environment in a vicinity of the Tyr and Trp residues and has several advantages, such as sensitivity, spectral simplification, spectral bandwidth reduction and avoiding different perturbing effects. According to the theory of Miller [41], when the D-value ($\Delta\lambda$) between excitation and emission wavelength is stabilized at 15 or 60 nm, the synchronous fluorescence gives the characteristic information of Tyr or Trp residues. The effect of C.I. Acid Red 2 on HSA synchronous fluorescence spectra is shown in Fig. 10. It can be seen from Fig. 10 that the maximum emission wavelength kept at the position when $\Delta\lambda$ = 15 nm, while a faint red shift can be observed when $\Delta\lambda$ = 60 nm. The faint red shift effect expresses the change in conformation of HSA. It is also indicated that the polarity around the Trp residue was increased and the hydrophobicity was decreased [42]. Furthermore, the fluorescence intensity decreased regularly with the addition of dye in both figures, which further illustrated the occurrence of fluorescence quenching in the binding process.

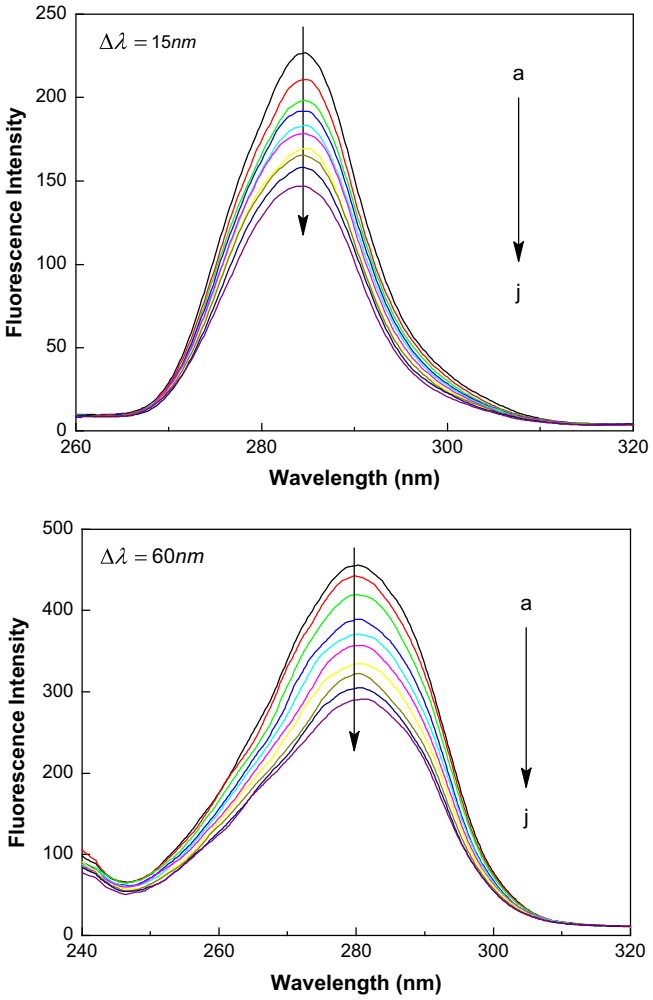

Fig. 10. Synchronous fluorescence spectrum of HSA in the absence and presence of C.I. Acid Red 2 (pH = 7.4, T = 298 K). (a) 1.0×10^{-6} M HSA; (b→j) 1.0×10^{-6} M HSA in the presence of 1.6, 3.2, 4.8, 6.4, 8.0, 9.6, 11.2, 12.8, 14.4 $\times$ 10^{-6} M C.I. Acid Red 2, respectively.

3.6.2. Electronic absorption spectra

Electronic absorption spectroscopy is a very simple method and applicable to explore the structural change and know the complex formation. In this work, the absorption spectra of HSA with various amounts of dye were recorded. Fig. 11 shows the absorption spectra of HSA from 240 to 325 nm in Tris–HCl buffer solution in the presence of different dye concentrations. It is evident that the absorbance of HSA decreased regularly with the variation of dye concentrations and the maximum peak position of dye–HSA was shifted from 275 to 271 nm. A reasonable explanation for the two observations may come from the interaction between dye and HSA. This also indicated that the peptide strands of the HSA molecules extend upon the addition of dye to HSA [43,44].

3.6.3. Circular dichroism

To further verify the secondary structure change of HSA when exposed to the dye, CD was employed on HSA and the HSA–dye complex. The raw CD spectra of HSA in the absence and presence

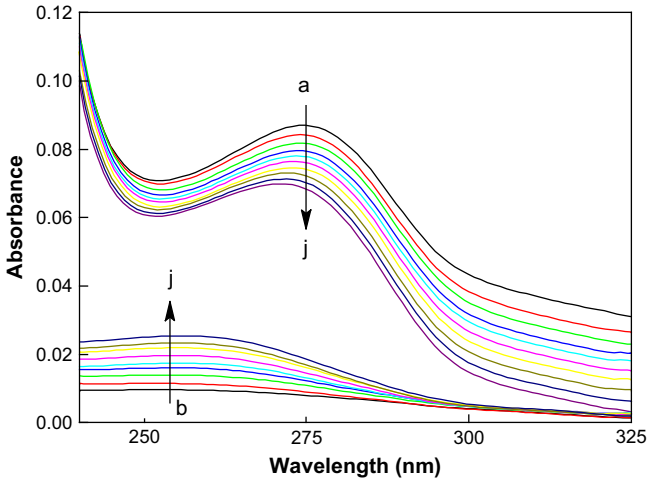

Fig. 11. UV–vis absorption spectra of HSA. HSA concentration was at 1.0×10^{-6} M (a) and C.I. Acid Red 2 concentration was at 1.6, 3.2, 4.8, 6.4, 8.0, 9.6, 11.2, 12.8, 14.4×10^{-6} M (b→j); pH = 7.4, T = 298 K.

of dye are shown in Fig. 12. The CD spectra of the HSA exhibited two negative bands at 208 and 222 nm, which are characteristic features of an α-helical protein structure. [45]. A reasonable explanation is that the negative peaks between 208 and 209 nm and 222 and 223 nm are both contributed by $n \rightarrow \pi^*$ transition for the peptide bond of α-helix [46]. The binding of dye to HSA caused only a decrease in band intensity without any significant shift of the peaks, clearly indicating that dye induced a slight decrease in the α-helical structure content of HSA. The α-helical content of HSA was calculated from equation (1) and the results displayed a reduction of α-helical structure from 35.84% to 34.57% at a molar ratio of HSA to dye of 1:4. From the above results, it was apparent that the effect of the dye on the HSA caused a secondary structure change of the protein, with the loss of helical stability.

3.6.4. Three-dimensional fluorescence spectra

Three-dimensional fluorescence spectroscopy has become a popular technique in recent years. The outstanding advantage of three-dimensional fluorescence spectra is that information regarding the fluorescence characteristics can be entirely acquired by changing excitation and emission wavelength simultaneously [47]. The three-dimensional fluorescence spectra of HSA and dye–HSA complex are shown in Fig. 13, and the corresponding characteristic parameters are listed in Table 4. As shown in Fig. 13, peak *a* is the Rayleigh scattering peak ($\lambda_{ex} = \lambda_{em}$) and peak *b* is the second-ordered scattering peak ($\lambda_{em} = 2\lambda_{ex}$) [48]. The fluorescence intensity of peak *a* and peak *b* increased with the addition of dye. The possible reason is that a dye–HSA complex came into being after the addition of dye, increasing the diameter of the macromolecule which in turn resulted in an enhanced scattering effect. Peak *1* mainly reveals the spectral behavior of Trp and Tyr residues. The reason is that when HSA is excited at 280 nm, it mainly reveals the intrinsic fluorescence of Trp and Tyr residues. Beside peak *1*, there is another fluorescence peak *2* (λ_{ex} = 230.0 nm, λ_{em} = 340.0 nm) that mainly reflects the fluorescence spectral behavior of the polypeptide backbone structure of HSA [49]. The fluorescence intensity of peak *2* decreased after the addition of dye, which means that the peptide strands structure of HSA has been changed. Analyzing from the fluorescence intensity changes of peak *1* and peak *2*, which decrease but to a different degree: in the absence and presence of dye, the intensity ratio of peak *1* and peak *2* was 1.08:1 and 1.23:1, respectively. The decrease of fluorescence intensity of the two peaks in combination with synchronous fluorescence, electronic absorption and CD results indicated that the interaction of dye with HSA induced a secondary structure change of HSA. The above phenomenon and analyzing of peak *1* and peak *2* revealed

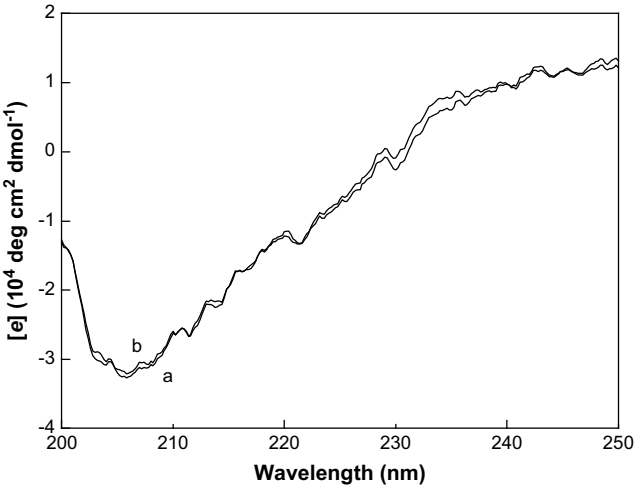

Fig. 12. CD spectra of the C.I. Acid Red 2–HSA system. (a) 1.0×10^{-6} M HSA; (b) 1.0×10^{-6} M HSA + 4.0×10^{-6} M C.I. Acid Red 2; pH = 7.4, T = 298 K.

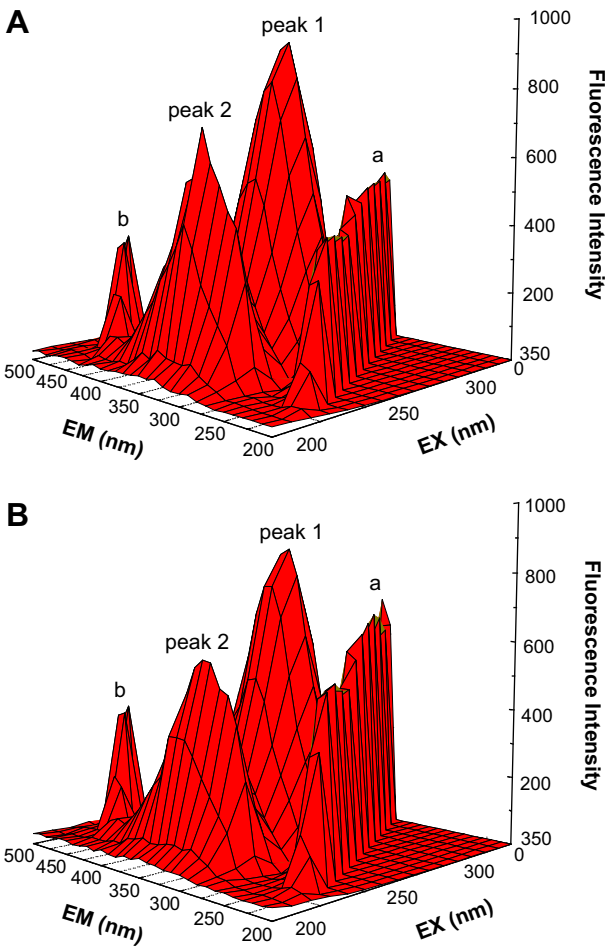

Fig. 13. Three-dimensional fluorescence spectra of HSA (A) and the C.I. Acid Red 2–HSA system (B). (A): c(HSA) = 3.0×10^{-6} M, c(C.I. Acid Red 2) = 0; (B): c(HSA) = 3.0×10^{-6} M, c(C.I. Acid Red 2) = 3.0×10^{-6} M pH = 7.4, T = 298 K.

Table 4
Three-dimensional fluorescence spectral characteristics of HSA and C.I. Acid Red 2–HSA system.

Peaks	HSA			C.I. Acid Red 2–HSA		
	Peak position $\lambda_{ex}/\lambda_{em}$ (nm/nm)	Stokes $\Delta\lambda$ (nm)	Intensity F	Peak position $\lambda_{ex}/\lambda_{em}$ (nm/nm)	Stokes $\Delta\lambda$ (nm)	Intensity F
Rayleigh scattering peaks	235/235→350/350	0	194.2→479.6	235/235→350/350	0	218.5→710.3
Fluorescence peak *1*	280.0/342.0	62.0	928.1	280.0/344.0	64.0	861.9
Fluorescence peak *2*	230.0/340.0	110.0	699.0	230.0/340.0	110.0	567.6

that the binding of C.I. Acid Red 2 to HSA induced some microenvironment and conformational changes in HSA.

3.7. Further considerations

Proteins with one polypeptide chain are monomeric proteins. Proteins composed of more than one polypeptide chain are multimeric proteins. In these multimeric proteins, the individual polypeptide chains are termed monomer or subunit [50]. Hydrogen bonds and electrostatic bonds formed between surface residues of adjacent subunits stabilize the association of subunits. Lyophilized HSA usually has covalent dimer structure (formed between mercapto residues during lyophilization). Furthermore, there is evidence in the literature that HSA can form noncovalent dimers as a function of concentration [51,52]. In this work, hydrogen bonds played major roles in the dye–HSA binding reaction, and the conformational changes occurring after the binding of dye, affecting the association between the dimer subunits, so this could be a state of association which changes as the HSA concentration is changed. Similar findings have also been reported by Levi and Flecha [53] for the binding of fluorescein-5′-isothiocyanate and eosin-5′-isothiocyanate with bovine serum albumin. All these aspects have to be taken into account because they affect binding results.

4. Conclusions

This paper presents spectroscopic investigation on the interaction of C.I. Acid Red 2 with HSA using fluorescence emission, synchronous fluorescence, electronic absorption, CD and three-dimensional fluorescence spectra. The experimental results indicated that the probable mechanism of C.I. Acid Red 2 interaction with HSA is a static quenching process. The binding of C.I. Acid Red 2 to HSA was found to be spontaneous and hydrophobic and hydrogen bond interactions played major role in the binding reaction. A site marker competitive experiment suggested that C.I. Acid Red 2 bound to the subdomain IIA of HSA (Sudlow's site I). The distance $r = 3.91$ nm between HSA and dye was obtained according to fluorescence resonance energy transfer. In the conformational investigation, synchronous fluorescence, electronic absorption, CD and three-dimensional fluorescence spectra revealed that the conformation and microenvironment of HSA were changed in the presence of C.I. Acid Red 2. The binding study of C.I. Acid Red 2 to HSA is greatly important in toxicology. This study provides important insight into the interactions of the physiological important protein HSA with azo dyes. Information is also obtained about azo dye induced secondary structure changes of HSA, which may be correlated to its physiological activity.

Acknowledgements

The authors are grateful to Professor Yurong Ma of College of Chemistry and Molecular Engineering, Peking University, for her constant support and expert assistance during the CD measurement experiments. Thanks are also due to Professor Haixiang Gao of Department of Chemistry, China Agricultural University, for his helpful suggestions in the preparation of this manuscript.

References

[1] Kim S-Y, An J-Y, Kim B-W. The effects of reductant and carbon source on the microbial decolorization of azo dyes in an anaerobic sludge process. Dyes and Pigments 2008;76(1):256–63.
[2] Fernandes A, Morão A, Magrinho M, Lopes A, Gonçalves I. Electrochemical degradation of C.I. Acid Orange 7. Dyes and Pigments 2004;61(3):287–96.
[3] Yilmaz A, Yilmaz E, Yilmaz M, Bartsch RA. Removal of azo dyes from aqueous solutions using calix[4]arene and β-cyclodextrin. Dyes and Pigments 2007;74(1):54–9.
[4] Medvedev ZA, Crowne HM, Medvedeva MN. Age related variations of hepatocarcinogenic effect of azo dye (3'-MDAB) as linked to the level of hepatocyte polyploidization. Mechanisms of Ageing and Development 1988;46(1–3):159–74.
[5] Percy AJ, Moore N, Chipman JK. Formation of nuclear anomalies in rat intestine by benzidine and its biliary metabolites. Toxicology 1989;57(2):217–23.
[6] Pardo O, Yusà V, León N, Pastor A. Development of a method for the analysis of seven banned azo-dyes in chilli and hot chilli food samples by pressurized liquid extraction and liquid chromatography with electrospray ionization-tandem mass spectrometry. Talanta 2009;78(1):178–86.
[7] Vijaya PP, Sandhya S. Decolorization and complete degradation of methyl red by a mixed culture. The Environmentalist 2003;23(2):145–9.
[8] Lachheb H, Puzenat E, Houas A, Ksibi M, Elaloui E, Guillard C, et al. Photocatalytic degradation of various types of dyes (Alizarin S, Crocein Orange G, methyl red, Congo red, Methylene Blue) in water by UV-irradiated titania. Applied Catalysis B: Environmental 2002;39(1):75–90.
[9] Gupta AK, Pal A, Sahoo C. Photocatalytic degradation of a mixture of Crystal Violet (Basic Violet 3) and methyl red dye in aqueous suspensions using Ag^+ doped TiO_2. Dyes and Pigments 2006;69(3):224–32.
[10] Abou-Zied OK, Al-Shihi OI. Characterization of subdomain IIA binding site of human serum albumin in its native, unfolded, and refolded states using small molecular probes. Journal of the American Chemical Society 2008;130(32):10793–801.
[11] He XM, Carter DC. Atomic structure and chemistry of human serum albumin. Nature 1992;358(6383):209–15.
[12] Sugio S, Kashima A, Mochizuki S, Noda M, Kobayashi K. Crystal structure of human serum albumin. Protein Engineering Design & Selection 1999;12(6):439–46.
[13] Kragh-Hansen U, Chuang VTG, Otagiri M. Practical aspects of the ligand-binding and enzymatic properties of human serum albumin. Biological & Pharmaceutical Bulletin 2002;25(6):695–704.
[14] Barbero N, Barni E, Barolo C, Quagliotto P, Viscardi G, Napione L, et al. A study of the interaction between fluorescein sodium salt and bovine serum albumin by steady-state fluorescence. Dyes and Pigments 2009;80(3):307–13.
[15] An WT, Jiao Y, Dong C, Yang C, Inoue Y, Shuang SM. Spectroscopic and molecular modeling of the binding of *meso*-tetrakis(4-hydroxyphenyl) porphyrin to human serum albumin. Dyes and Pigments 2009;81(1):1–9.
[16] Yue YY, Chen XG, Qin J, Yao XJ. Characterization of interaction between C.I. Acid Green 1 and human serum albumin: spectroscopic and molecular modeling method. Dyes and Pigments 2009;83(2):148–54.
[17] Shaikh SMT, Seetharamappa J, Ashoka S, Kandagal PB. A study of the interaction between bromopyrogallol red and bovine serum albumin by spectroscopic methods. Dyes and Pigments 2007;73(2):211–6.
[18] Shaikh SMT, Seetharamappa J, Kandagal PB, Manjunatha DH, Ashoka S. Spectroscopic investigations on the mechanism of interaction of bioactive dye with bovine serum albumin. Dyes and Pigments 2007;74(3):665–71.
[19] Yue YY, Chen XG, Qin J, Yao XJ. A study of the binding of C.I. Direct Yellow 9 to human serum albumin using optical spectroscopy and molecular modeling. Dyes and Pigments 2008;79(2):176–82.
[20] Klotz IM, Burkhard RK, Urquhart JM. Structural specificities in the interactions of some organic ions with serum albumin. Journal of the American Chemical Society 1952;74(1):202–8.
[21] Burkhard RK, Moore FA, Louloudes SJ. The interactions of the methyl reds and bovine serum albumin. Archives of Biochemistry and Biophysics 1961;94(2):291–300.

[22] Wallevik K. Reversible denaturation of human serum albumin by pH, temperature, and guanidine hydrochloride followed by optical rotation. The Journal of Biological Chemistry 1973;248(8):2650–5.
[23] Chen Y-H, Yang JT, Martinez HM. Determination of the secondary structures of proteins by circular dichroism and optical rotatory dispersion. Biochemistry 1972;11(22):4120–31.
[24] Papadopoulou A, Green RJ, Frazier RA. Interaction of flavonoids with bovine serum albumin: a fluorescence quenching study. Journal of Agricultural and Food Chemistry 2005;53(1):158–63.
[25] Zhang HM, Wang YQ, Fei ZH, Wu L, Zhou QH. Characterization of the interaction between Fe(III)-2,9,16,23-tetracarboxyphthalocyanine and blood proteins. Dyes and Pigments 2008;78(3):239–47.
[26] Lakowicz JR. Principles of fluorescence spectroscopy. 3rd ed. New York: Springer Science+Business Media; 2006. p. 277.
[27] Lakowicz JR, Weber G. Quenching of fluorescence by oxygen. A probe for structural fluctuations in macromolecules. Biochemistry 1973;12(21):4161–70.
[28] Ware WR. Oxygen quenching of fluorescence in solution: an experimental study of the diffusion process. The Journal of Physical Chemistry 1962;66(3):455–8.
[29] Wang J, Zhang Y-Y, Guo Y, Zhang L, Xu R, Xing Z-Q, et al. Interaction of bovine serum albumin with Acridine Orange (C.I. Basic Orange 14) and its sonodynamic damage under ultrasonic irradiation. Dyes and Pigments 2009;80(2):271–8.
[30] Dong LJ, Chen XG, Hu ZD. Study on the binding of Arsenazo-TB to human serum albumin by Rayleigh light scattering technique and FT-IR. Biochimica et Biophysica Acta 2006;1764(2):257–62.
[31] Dong LJ, Chen XG, Hu ZD. Study of the effect of Cal-Red on the secondary structure of human serum albumin by spectroscopic techniques. Journal of Molecular Structure 2007;846(1–3):112–8.
[32] Tinoco AD, Eames EV, Incarvito CD, Valentine AM. Hydrolytic metal with a hydrophobic periphery: titanium(IV) complexes of naphthalene-2,3-diolate and interactions with serum albumin. Inorganic Chemistry 2008;47(18):8380–90.
[33] Gharagozlou M, Boghaei DM. Interaction of water-soluble amino acid Schiff base complexes with bovine serum albumin: fluorescence and circular dichroism studies. Spectrochimica Acta Part A: Molecular and Biomolecular Spectroscopy 2008;71(4):1617–22.
[34] Klotz IM. Physicochemical aspects of drug-protein interactions: a general perspective. Annals of the New York Academy of Sciences 1973;226(Part I):18–35.
[35] Ross PD, Subramanian S. Thermodynamics of protein association reactions: forces contributing to stability. Biochemistry 1981;20(11):3096–102.
[36] Bi SY, Ding L, Tian Y, Song DQ, Zhou X, Liu X, et al. Investigation of the interaction between flavonoids and human serum albumin. Journal of Molecular Structure 2004;703(1–3):37–45.
[37] Sudlow G, Birkett DJ, Wade DN. The characterization of two specific drug binding sites on human serum albumin. Molecular Pharmacology 1975;11(6):824–32.
[38] Förster T. Zwischenmolekulare Energiewanderung und Fluoreszenz. Annalen der Physik 1948;437(1–2):55–75.
[39] Förster T, Sinanoglu O. Modern quantum chemistry, vol. 3. New York: Academic Press; 1996. p. 93.
[40] Lloyd JBF, Evett IW. Prediction of peak wavelengths and intensities in synchronously excited fluorescence emission spectra. Analytical Chemistry 1977;49(12):1710–5.
[41] Miller JN. Recent advances in molecular luminescence analysis. Proceeding of the Analytical Division of the Chemical Society 1979;16(7):203–8.
[42] Yuan T, Weljie AM, Vogel HJ. Tryptophan fluorescence quenching by methionine and selenomethionine residues of calmodulin: orientation of peptide and protein binding. Biochemistry 1998;37(9):3187–95.
[43] Kandagal PB, Shaikh SMT, Manjunatha DH, Seetharamappa J, Nagaralli BS. Spectroscopic studies on the binding of bioactive phenothiazine compounds to human serum albumin. Journal of Photochemistry and Photobiology A: Chemistry 2007;189(1):121–7.
[44] Kandagal PB, Kalanur SS, Manjunatha DH, Seetharamappa J. Mechanism of interaction between human serum albumin and N-alkyl phenothiazines studied using spectroscopic methods. Journal of Pharmaceutical and Biomedical Analysis 2008;47(2):260–7.
[45] Greenfield NJ. Determination of the folding of proteins as a function of denaturants, osmolytes or ligands using circular dichroism. Nature Protocols 2006;1(6):2733–41.
[46] Kelly SM, Jess TJ, Price NC. How to study proteins by circular dichroism. Biochimica et Biophysica Acta 2005;1751(2):119–39.
[47] Rodríguez-Cuesta MJ, Boqué R, Rius FX, Zamora DP, Galera MM, Frenich AG. Determination of carbendazim, fuberidazole and thiabendazole by three-dimensional excitation-emission matrix fluorescence. Analytical Chimica Acta 2003;491(1):47–56.
[48] Zhang YZ, Chen XX, Dai J, Zhang XP, Liu YX, Liu Y. Spectroscopic studies on the interaction of lanthanum(III) 2-oxo-propionic acid salicyloyl hydrazone complex with bovine serum albumin. Luminescence 2008;23(3):150–6.
[49] Wang YQ, Tang BP, Zhang HM, Zhou QH, Zhang GC. Studies on the interaction between imidacloprid and human serum albumin: spectroscopic approach. Journal of Photochemistry and Photobiology B: Biology 2009;94(3):183–90.
[50] Murray RK, Granner DK, Mayes PA, Rodwell VW. Harper's biochemistry. 25th ed. New York: McGraw-Hill Companies; 2000. p. 48.
[51] Jin RZ, Karol MH. Intra- and intermolecular reactions of 4,4'-diisocyanatodiphenylmethane with human serum albumin. Chemical Research in Toxicology 1988;1(5):281–7.
[52] Martinez-Landeira P, Ruso JM, Prieto G, Sarmiento F, Jones MN. The interaction of human serum albumin with dioctanoylphosphatidylcholine in aqueous solutions. Langmuir 2002;18(8):3300–5.
[53] Levi V, Flecha FLG. Reversible fast-dimerization of bovine serum albumin detected by fluorescence resonance energy transfer. Biochimica et Biophysica Acta 2002;1599(1-2):141–8.